Direct numerical simulation of the development of asymmetric perturbations at very late stages of the transition process

Daniel G.W. Meyer, Ulrich Rist, and Siegfried Wagner

IAG, Universität Stuttgart, Pfaffenwaldring 21, 70550 Stuttgart, Germany
`daniel.meyer@iag.uni-stuttgart.de`,
WWW home page:
`http://www.iag.uni-stuttgart.de/people/daniel.meyer/`

Summary

An investigation on the development of asymmetric perturbations at extremely late stages of the transition process, right before the boundary layer becomes fully turbulent, will be presented. The influence of asymmetric disturbances on the time averaged flow and the local flow dynamics close to the original symmetry plane will be demonstrated. We introduce small asymmetric disturbances which mimic small-amplitude random background perturbations that are present in any realistic flow situation. We focus on how the flow is transformed from a symmetric to an asymmetric one by these additional perturbations, and we try to identify instability mechanisms which are responsible for the amplification of these asymmetric disturbances. Thus, the aim of the present investigations is to contribute to a deeper understanding of turbulence production.

1 Introduction

In previous work we performed combined experimental and numerical studies of the influence of the generic Λ-structure on the surrounding flow field (see [1] and [2]), and the flow randomization process beginning when the first spikes are observed in the flow field (see [3]). These investigations were restricted to stages of the transition process that are already dominated by strongly nonlinear developments, but the number of distinct coherent structures in the boundary layer was still small. Going only a little further downstream we face a fully developed turbulent boundary layer which is completely filled up with a huge number of interacting vortices and shear layers. The current work is concerned with the investigation of these extremely late stages of the transition process. The computations are based on the carefully validated simulations presented in [3]. The numerical method used is described in detail in [4].

In order to provide an idea of the huge number of vortices present in the boundary layer at the very late stages of transition, figure 1 shows a vortex visualization at these stages using the λ_2-method as described in [5]. Compare the number of
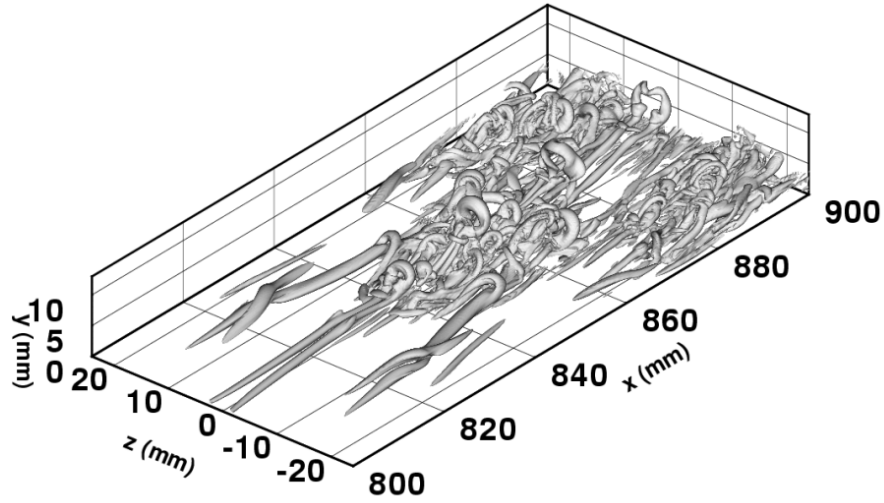
Figure 1 λ_2 vortex visualization right before the boundary layer becomes fully turbulent. Wavelength of the fundamental wave $\lambda_{TS} \approx 43$ mm. DNS data taken from [3].

small-scale structures with the wavelength $\lambda_{TS} \approx 43$ mm of the fundamental 2D TS-wave that is used to initiate this K-Type breakdown process! Using a DNS code for spatial simulations, the calculations were performed with a symmetric spectral ansatz with respect to $z = 0$ in spanwise direction, because the disturbance input was also symmetric in that case. From experiments we know that the late stages of the transition process are very sensitive to background perturbations and that the flow structures tend to become asymmetric despite a completely symmetric disturbance input. This poses some questions: Should symmetric calculations, which have many times proven to be very useful at earlier stages of the transition process, still be applied for very late stages of the transition process, or do we have to permit an asymmetric development of the flow in order to get meaningful results? How exactly do asymmetric disturbances influence the flow? Are there any significant instability mechanisms that are suppressed by the symmetry assumption?

2 Influence of asymmetric perturbations on late-stage transition

In order to investigate these questions we expanded a symmetric DNS to an asymmetric one by adding the missing real or imaginary parts of the spectral ansatz. Afterwards, the calculations were continued with the extended ansatz. If the additional terms in the ansatz are initialized with zero values and if we continue to introduce only symmetric disturbances into the flow, it will remain completely symmetric. But when we initialize the additional terms with very small random values with dimen-
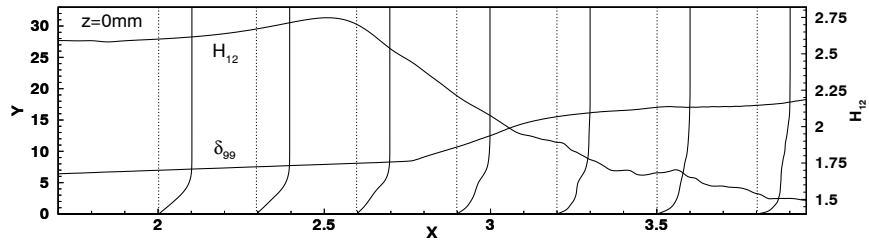
Figure 2 Development of the time averaged boundary layer thickness δ_{99}, the u-velocity profiles and the shape factor H_{12} in the peak plane at $z = 0$.

sionless amplitudes of about 10^{-12}, we observe that the asymmetric perturbations grow very fast by several orders of magnitude (up to 10^{-6} in the current DNS), at the very late stages of transition ($H_{12} \leq 1.8$) before they are convected out of the integration domain and hence the flow becomes symmetric again. This suggests that the very late stages are convectively unstable with respect to these asymmetric perturbations. In order to study this instability in more detail, we introduced controlled asymmetric perturbations into the boundary layer by suction and blowing via a second disturbance slot.

Figure 2 provides an overview of the development of some time averaged boundary layer parameters in the peak plane at $z = 0$. The x-range of the data shown in figure 1 corresponds to $3.05 \leq x \leq 3.55$ in dimensionless coordinates. The center of the disturbance slot for adding asymmetric perturbation is located at $x \approx 2.95$. Figure 3 shows the amplitude distribution of the asymmetric disturbance versus the spanwise direction on the left hand side. It is created by superposing four pairs of oblique waves ($1 \leq k \leq 4$) that have a spanwise phase of $\frac{\pi}{2}$ and can therefore only be represented by a complete spectral ansatz without symmetry assumption (v usually has a $\cos$-shaped distribution vs. z). All wave pairs have a v-amplitude of 10^{-5}
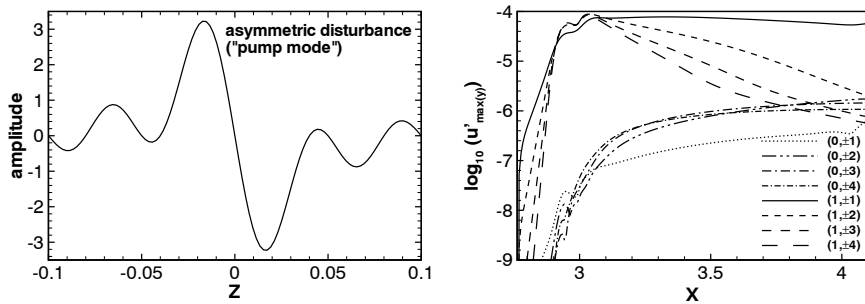
Figure 3 Left: asymmetric v amplitude distribution vs. z (pump mode). Right: u amplification curves resulting from disturbing the laminar base flow with the pump mode.

and are generated with the fundamental frequency. Thus, the amplitude distribution shown in figure 3 fluctuates in time and causes alternating suction and blowing at each side of the peak plane. The maxima of the amplitude distribution are located close to the legs of the Λ-vortices that are convected above the disturbance slot in the boundary layer. On the right hand side of figure 3 the amplitude development of the disturbances which are generated by introducing the pump mode into the otherwise undisturbed laminar base flow can be observed. All fluctuating modes decay while the steady base flow deformations grow weakly on a very low amplitude level. However, the important point is that the asymmetric pump mode itself does not initiate transition in an otherwise undisturbed laminar boundary layer.

In order to get an impression of the amplification of asymmetric disturbances during the transition process we need a quantitative measure to describe asymmetric growth. One such measure is the w-velocity component in the peak plane at $z = 0$, because this quantity is zero in symmetric calculations. It can only become non-zero in an asymmetric case and is therefore a direct measure for asymmetry in the flow. Here we will use the wall-normal maximum of the time averaged w-component at each x-position. In figure 4 the growth of the w-amplitude in downstream direction is shown for two cases: The lower curves clearly indicate that asymmetry decays when the pump mode is introduced in the otherwise undisturbed laminar boundary layer. In contrast to that, the upper curves indicate that asymmetry strongly grows when the pump mode is introduced into the boundary layer at very late stages of the transition process which is caused by purely symmetric disturbances. Despite the low amplitude level at which the additional perturbations are generated, we find instantaneous w-amplitudes of up to $0.2U_\infty$ in the original symmetry plane at $z = 0$. The strong growth of these disturbances begins at $x \approx 3.4$ when the boundary layer is already filled up with a huge number of small-scale vortices that seem to inter-
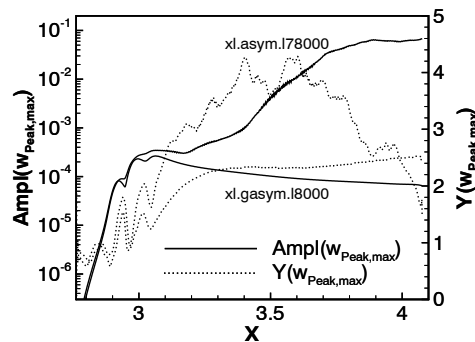
Figure 4   Growth of the w-velocity component (solid lines) and wall-normal location of the w-maxima (dotted lines) in the peak plane. Lower curves: laminar base flow disturbed using the pump mode. Upper curves: pump mode used to introduce asymmetric perturbations into an otherwise only symmetrically disturbed boundary layer at late stages of the transition process.

act with each other and thus contribute to the spreading of asymmetric disturbances throughout the boundary layer. The positions of the extrema in the latter case are at first located quite far away from the wall in the outer part of the boundary layer and then move closer towards the wall when the boundary layer becomes fully turbulent. This suggests that the initial asymmetric fluctuations are linked to the coherent structures in the outer part of the boundary layer.

Figure 5 displays how the time averaged velocity field at $x = 4.05$ is affected by the symmetry condition. The $\overline{v}$- and $\overline{w}$-components show only minor differences, whereas the $\overline{u}$-component is significantly changed by the symmetry assumption. Around $z = 0$, in the vicinity of the original symmetry plane, the spanwise gradients are much less emphasized in the asymmetric case. This points to a notice-
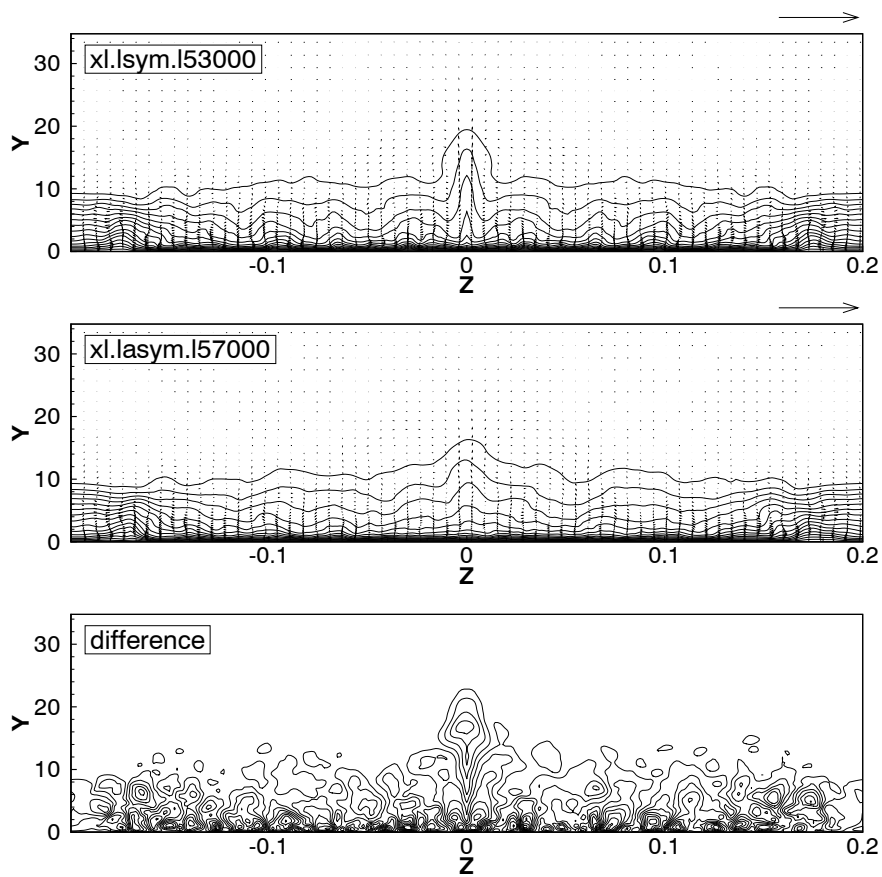
Figure 5 Time averaged velocity components for a symmetric case (top), an asymmetric case (middle) and the difference $\Delta \overline{u}$ (bottom) of the u-velocity component at $x = 4.05$. 15 isovalues in the range $-0.122 \leq \Delta \overline{u} \leq 0.101$. Reference vetor U_∞. Aspect ratio $y : z = 1$.

able change in local flow dynamics of the almost turbulent flow, which is obviously strongly dependent on the choice of allowing or suppressing spanwise fluctuations at $z = 0$. Interestingly, the largest differences do not occur at the spike positions in the outer part of the boundary layer where we find the strongest instantaneous gradients in the flow ($\Delta \overline{u}$ up to $0.06 U_\infty$), but close to the wall where strong time averaged velocity gradients prevail ($\Delta \overline{u}$ locally up to $0.13 U_\infty$). The $\overline{u}$-profile of the asymmetric simulation is not as strongly modulated in spanwise direction as in the symmetric case. When looking at boundary layer parameters that are averaged in time and spanwise direction, like the shape factor or the wall shear stress, the symmetric and asymmetric simulations differ only slightly, with the symmetric simulation showing a tendency to a faster development.

In figure 6 the time averaged velocity profiles are shown at $x = 4.05$ and three different spanwise positions together with the total u_{rms}-profiles in order to reveal the local dynamics in the boundary layer for the symmetric as well as the asymmetric case. The largest differences are found in the peak plane at $z = 0$. Here, the time averaged profiles and the u_{rms}-profiles differ strongly. Particularly the differences in the u_{rms}-profiles indicate a complete modification of local flow dynamics. At the other two spanwise positions we find somewhat smaller differences between the two cases. For other z-positions (not shown), the differences are in general comparable to the off-peak positions chosen here.

Figure 7 compares the w-fluctuations in the peak plane with a projection of the λ_2-data which helps to recognize the relative positions of the coherent vortical motion and the asymmetric fluctuations. Most of the spanwise fluctuations occur in the vicinity of the vortices close to the peak plane, especially at positions that correspond to the legs which connect neighboring Ω-shaped or ring-like vortices. This indicates that, most likely, the mechanism of growth of asymmetric disturbances is connected to the development of these vortices in the boundary layer.
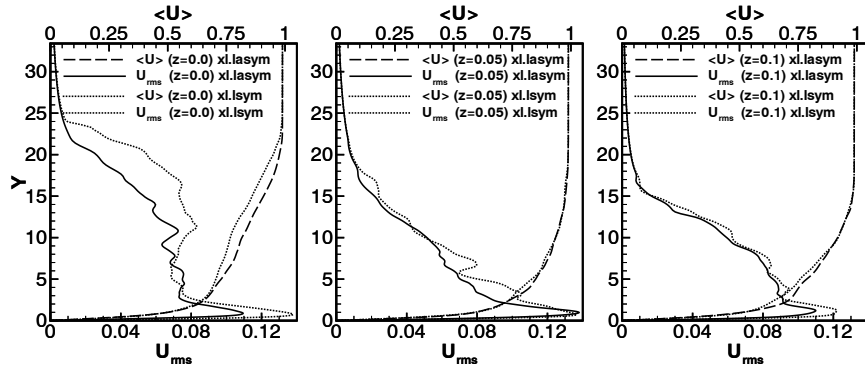
Figure 6 Comparison of symmetric and asymmetric simulations. Time averaged u-profiles and u_{rms}-profiles at $x = 4.05$ at three different z-positions.
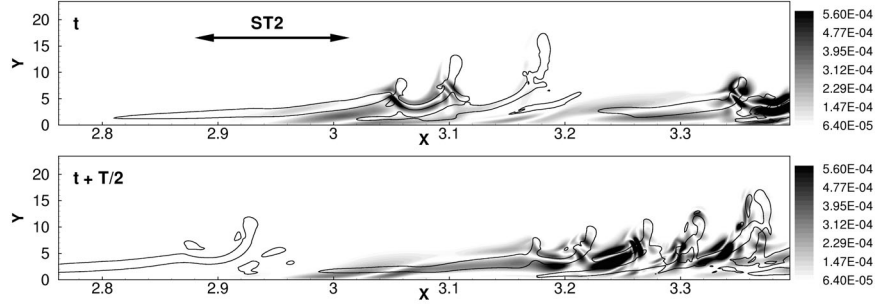
Figure 7 w-fluctuations in the peak plane correlate largely with the vortical structures in the boundary layer. $\sqrt{\overline{w^2}}|_{z=0}$ as grey scale together with a λ_2-projection (isolines). Asymmetric disturbance input at the second disturbance slot ST2 located at the wall.

The results presented up to now seem to suggest that the local development of the flow in the vicinity of the peak plane is severely restricted by the symmetry condition at very late stages of the transition process, and that the development of the asymmetric perturbations is coupled to the downstream evolution of the vortices in the flow field. Therefore, we will try to use vortex visualizations to compare the behavior in both cases. Figures 8 to 11 show comparisons of λ_2-visualizations of instantaneous flow field data for the symmetric and the asymmetric case at the same time step. Figure 2 can be used in order to get a reference to the stage of the transition process that corresponds to the x-range shown in each picture.

In figure 8 a perspective view of the vortices in both cases is shown. The boundary layer is already filled with many vortices at this stage of the development. At a first glance, we can see identical vortices in both cases, but close to the original peak plane there are noticeable differences between symmetric and asymmetric simulation (marked by arrows). The legs of the Ω-vortex extending roughly in upstream direction from the Ω-shaped vortex towards the wall are already broken down in the asymmetric case. This can be seen even better in the top view visualization in figure 9 where the vicinity of the original symmetry plane is marked by a black frame. The forced symmetry is plainly visible in the upper plot, leading to virtually parallel vortices on each side of the symmetry plane, whereas a meandering motion of the legs of the Ω-vortices in the asymmetric case and a tendency of these vortices to break down into smaller vortices can be recognized by comparing both plots. Further away from z=0 in the asymmetric case in figure 9, the flow is still completely symmetric, i.e., the asymmetric fluctuations did not yet spread very far in spanwise direction away from the original symmetry plane.

Figure 10 demonstrates that, in addition to the breakdown of the Ω-legs as described above, there are other asymmetric deformations and displacements of the vortices in the asymmetric case that modify the flow field close to the original symmetry plane. On the left hand side in the region marked by a frame it can be seen how the Ω-shaped vortex loops deform in a way that one side of the loop is located
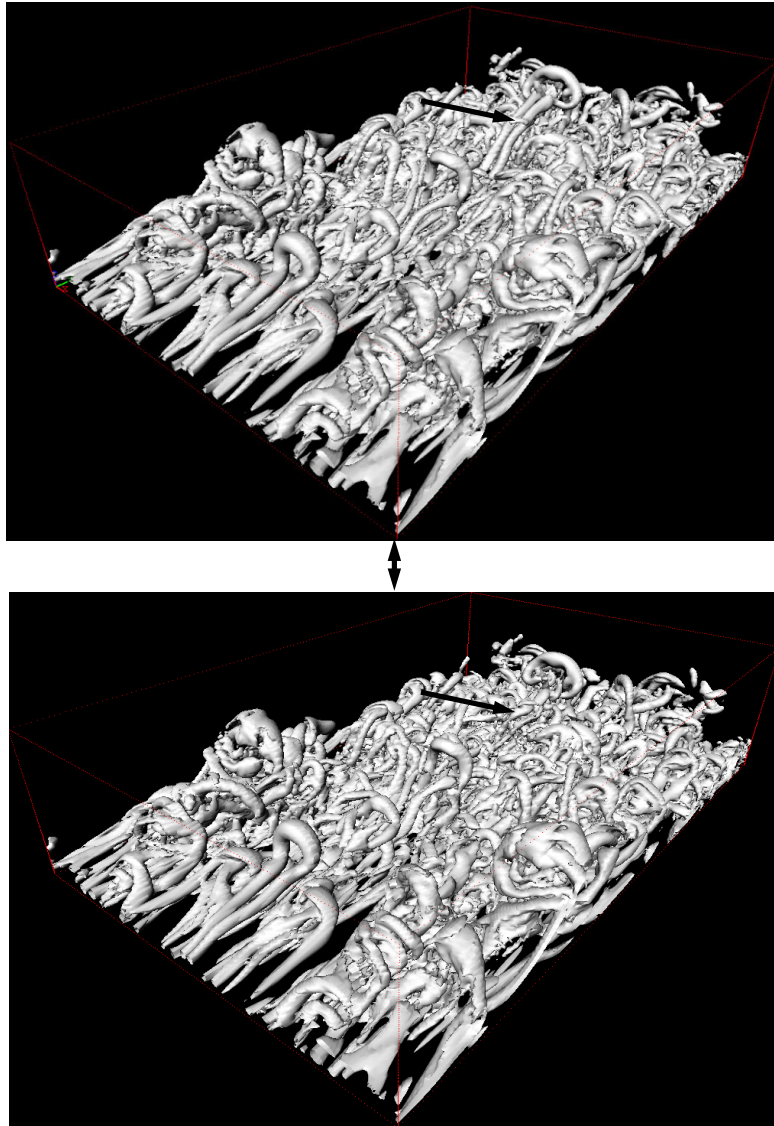
Figure 8 Comparison of symmetric (top) and asymmetric (bottom) simulation in the range $3.41 \le x \le 3.73$, $|z| \le 0.1$ using λ_2 vortex visualizations. Breakdown of the legs of the Ω-vortex for the asymmetric case in the vicinity of the original symmetry plane (indicated by arrows).

further downstream than the other side. The vortex thus becomes asymmetric with respect to the plane $z = 0$. Even further away from the old symmetry plane asym-

metric deformations become more emphasized (see the regions marked by circles). On the right hand side of figure 10 an additional possibility for a typical asymmetric development can be seen. Here, only one structure can be observed in the asymmetric case where two structures could be distinguished in the symmetric case, i.e., in the asymmetric case a coalescence of structures occurs that were clearly separated in the symmetric case.
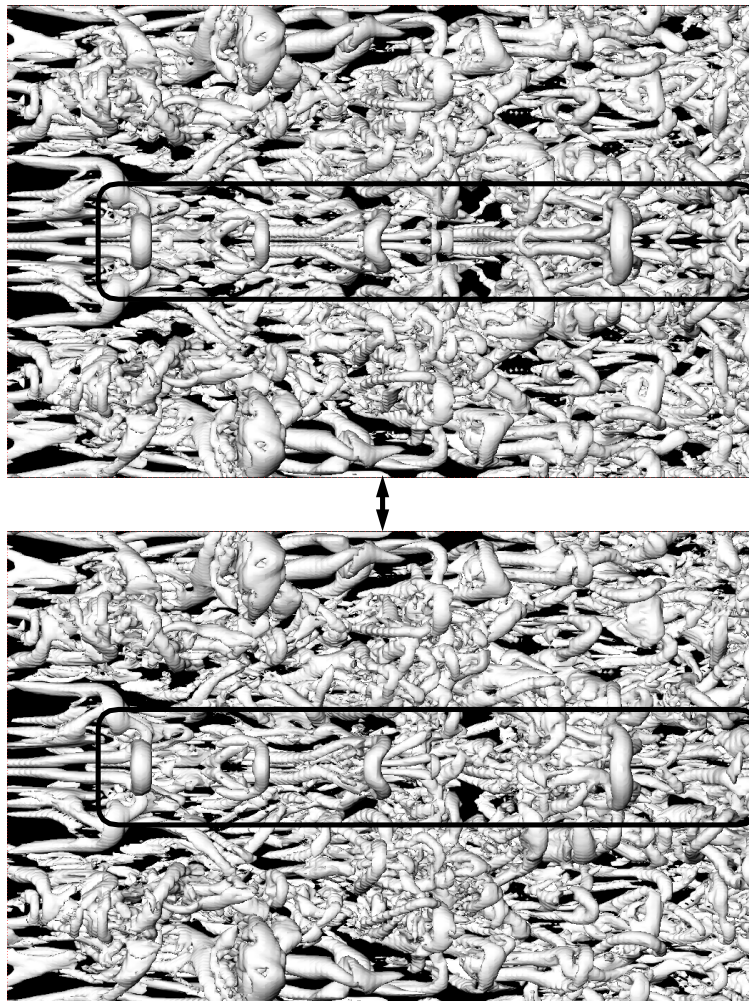
Figure 9   Same data and range as in figure 8. Symmetric case (top) and asymmetric case (bottom). Top view visualization.
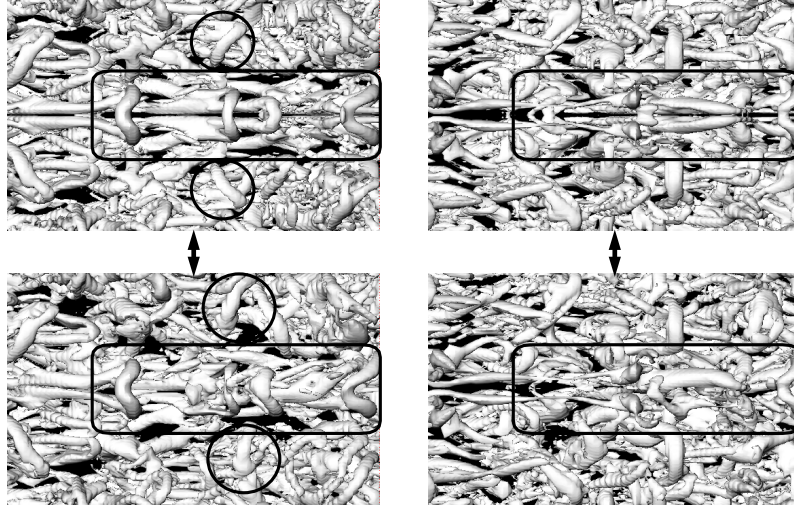
Figure 10   Comparison of symmetric (top) and asymmetric (bottom) simulation in the range $3.57 \leq x \leq 3.73$, $|z| \leq 0.05$ using top view λ_2 vortex visualizations. Different characteristic asymmetric deformations (bottom) compared with the symmetric case (top).

Going even further downstream than in the previous figures and comparing the instantaneous data of both cases (see figure 11), we observe that the flow field in the vicinity of the original symmetry plane has completely changed. The vortices look very different in both cases. Taking into account that the vortex legs are regions of strong local velocity gradients in the flow, the large differences in the time averaged u-profiles and in u_{rms}-profiles between both cases shown in figures 5 and 6 become understandable, as the position $x = 4.05$ corresponds to the right edge of figure 11. There is obviously a rather strong sensitivity of the flow development to background perturbations in the very late or nearly turbulent stages of the transition process which gives rise to a fast growth of any asymmetric fluctuations, i.e., the symmetry assumption is too restrictive and inhibits a realistic development of the flow at these late stages when small background perturbations are present. Further away from $z = 0$ it takes some time to identify corresponding vortical structures in both cases and one can clearly see that the details of the flow differ throughout the whole domain, but still some similarities can be identified.

3   Conclusions

We can summarize that a DNS in which a symmetry assumption for the flow development in spanwise direction is employed, does not seem to be adequate for simulating the very late, almost turbulent stages of the transition process. This is particularly true when we can expect that any asymmetric background perturbations are present in the boundary layer. The vortices in the flow would develop differently
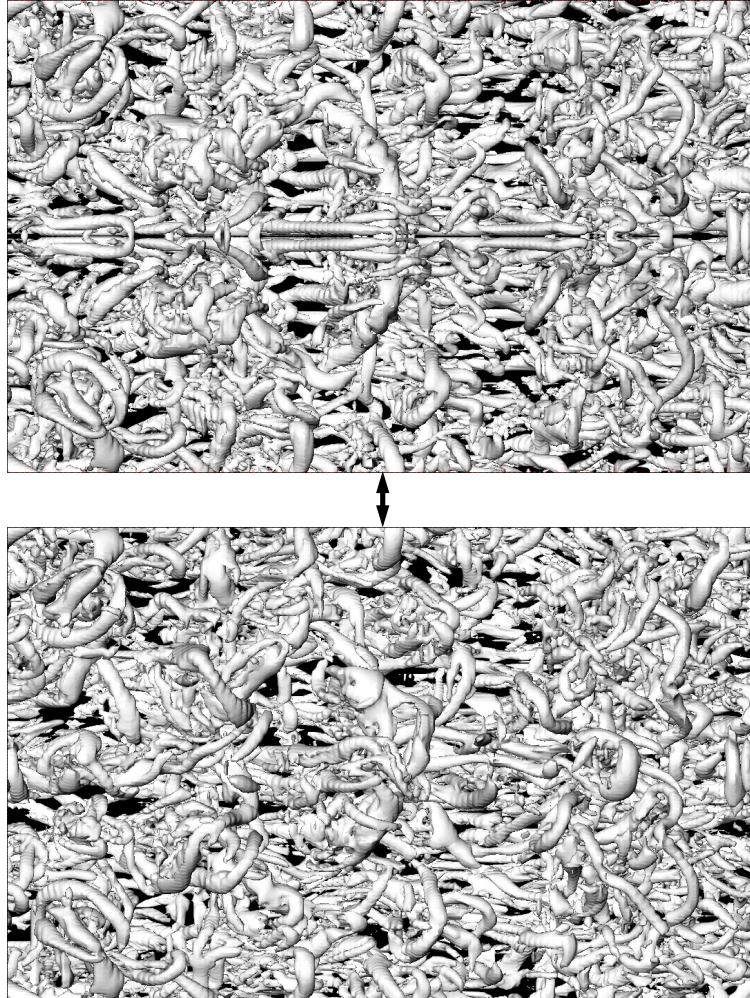
Figure 11 Comparison of symmetric (top) and asymmetric (bottom) simulation further downstream in the range $3.73 \leq x \leq 4.05$, $|z| \leq 0.1$ using top view λ_2 vortex visualizations.

at least in the vicinity of the original symmetry plane in an asymmetric simulation, triggered by the background perturbations. Local flow dynamics is changed significantly in the asymmetric case compared to the symmetric one, which can be clearly seen for time averaged as well as for total u_{rms}-profiles. Three typical differences could be identified: i) breakdown of the legs of the Ω-vortices by a meandering motion in spanwise direction, ii) spanwise as well as downstream displacement and deformation of vortices in the vicinity of the original symmetry plane, and iii) coalescence of structures in the asymmetric case that are separated in the symmetric

case on both sides of the symmetry plane. However, this becomes only relevant at the very late stages of the transition process when the boundary layer is already filled with a huge number of small-scale vortices. For the Blasius case studied here, we found that $H_{12} \leq 1.8$ is a necessary condition, but this might be strongly dependent on the amplitude level of the asymmetric background perturbations. The symmetry assumption seems to suppress certain degrees of freedom of the vortex evolution which are used and filled up very fast in an asymmetric simulation due to the permanent interactions between the many vortices in the boundary layer as soon as there is any external asymmetric perturbation that triggers this development.

The present study indicates that even very small external perturbations will significantly influence the instantaneous flow field and that any small initial asymmetry will grow quickly and spread over the whole flow field. Since the random background perturbations in an experiment are unknown by definition, it seems to be impractical to compare experimental and numerical results in more detail than looking at time averaged or $r.m.s.$-averaged values. In the near future the DNS will probably be the only means to study local flow dynamics in a (nearly fully developed) turbulent boundary layer under controlled and repeatable conditions.

Acknowledgements

References

[1] Meyer, D.G.W., Rist, U., Borodulin, V.I., Gaponenko, V.R., Kachanov, Y.S., Lian, Q.X., Lee, C.B.: Late-stage transitional boundary-layer structures. Direct numerical simulation and experiment. In Fasel, H., Saric, W., eds.: IUTAM Symposiom on Laminar-Turbulent Transition, Sedona, Az./USA, Springer (1999) 167–172

[2] Borodulin, V.I., Gaponenko, V.R., Kachanov, Y.S., Meyer, D.G.W., Rist, U., Lian, Q.X., Lee, C.B.: Late-stage transitional boundary-layer structures. Direct numerical simulation and experiment. Theor. Comput. Fluid Dynamics **15** (2002) 317–337

[3] Bake, S., Meyer, D.G.W., Rist, U.: Turbulence mechanism in Klebanoff-transition. A quantitative comparison of experiment and direct numerical simulation. J. Fluid Mech. **459** (2002) 217–243

[4] Meyer, D.: Direkte numerische Simulation nichtlinearer Transitionsmechanismen in der Strömungsgrenzschicht einer ebenen Platte. Dissertation, Universität Stuttgart (2002)

[5] Jeong, J., Hussain, F.: On the identification of a vortex. J. Fluid Mech. **285** (1995) 69–94